Applications and Applied Mathematics: An International Journal (AAM)

Volume 15 | Issue 2 Article 27

12-2020

Effect of Induced Magnetic Field on Mixed Convection Flow in a Vertical Channel with Symmetric and Asymmetric Wall Heating Conditions

Hasan N. Zaidi
University of Hail, KSA

Available at
http://pvamu.edu/aam
Appl. Appl. Math.
ISSN: 1932-9466

Applications and
Applied Mathematics:
An International Journal
(AAM)

Vol. 15, Issue 2 (December 2020), pp. 1172 - 1192

Effect of Induced Magnetic Field on Mixed Convection Flow in a Vertical Channel with Symmetric and Asymmetric Wall Heating Conditions

Hasan Nihal Zaidi

Department of Basic Science
College of Preparatory Year
University of Hail, KSA
hasannihalzaidi@hotmail.com

Received: March 11, 2020; Accepted: August 23, 2020

Abstract

The present paper concerns the study of the induced magnetic field effect on mixed convection flow of viscous incompressible electrically conducting fluid in a vertical channel with symmetric and asymmetric wall heating conditions with heat generation. A steady, laminar, and fully developed flow is considered. Through the appropriate choice of dimensionless variable, the governing equations are developed and three types of thermal boundary conditions isothermal-isothermal, isoflux-isothermal, and isothermal-isoflux for the left-right wall of the channel have prescribed. The analytical solutions for the velocity field, temperature field, magnetic field, and induced current density have been acquired for three types of thermal boundary conditions. A parametric study has been conducted and, the graphical results are exhibited for the velocity field, magnetic field, induced current density, and Nusselt number.

Keywords: Mixed convection; Induced magnetic field; Heat generation; Nusselt number; Induced current density

MSC 2010 No.: 76D05, 76E05, 76W05

Nomenclature

A	constant pressure gradient	ν	kinematic viscosity
D	$2L$, hydraulic diameter	μ	dynamic viscosity
g	acceleration due to gravity	ρ	fluid density
L	channel width	β	thermal expansion coefficient
$B_0^{'}$	constant strength of applied magnetic field	σ	fluid electrical conductivity
$B_x^{'}$	dimensional induced magnetic field	μ_e	magnetic permeability

B	dimensionless induced magnetic field define in Equation (5)	Gr	Grashof number
		Pr	Prandtl number
η	dimensionless parameter (Gr/Re) define in Equation (5)	Pm	magnetic Prandtl number
		M	Hartmann number
T	temperature	u'	dimensional velocity
T_1, T_2	prescribed boundary temperature	u	dimensionless velocity
ΔT	reference temperature difference	T_0	reference temperature
Q_0	heat generation coefficient	Re	Reynolds number
Rt	$=(T_2-T_1)/\Delta T$ temperature difference ratio	x', y'	space coordinates
θ	dimensionless temperature defined in Eq. (5)	J	induced current density
ϕ	heat generation coefficient defined in Eq. (5)		
P	$p+\rho gx$ difference between the pressure and hydrostatic pressure		

1. Introduction

During the last decades, the problems of mixed convection and heat transfer flow through a vertical channel have attracted the attention of several researchers because of its potential applications in numerous industrial and engineering applications such as cooling of electronic equipment, heating of Trombe wall system, gas-cooled nuclear reactors, geothermal reservoir, etc. Mixed convection flow occurs when both natural and forced convection mechanism simultaneously and significantly contribute to the heat transfer. Ostrach (1654) had been thoroughly explored, the steady laminar natural and forced convection flow and heat transfer of a viscous incompressible fluid in a vertical channel with and without heat sources considering linearly varying wall temperature. Aung and Worku (1986) have been investigated the theory of combined convection in a vertical channel along with flow reversal conditions. Also, Aung and Worku (1986, 1987) studied developing flow and flow reversal in a vertical channel with asymmetric wall temperature and the mixed convection flow in ducts with asymmetric wall heat flux. The heat transfer of fully developed mixed convection in a heated vertical channel with flow reversal phenomena has been analyzed by Cheng et al. (1990). Chamkha (2002) had investigated the hydromagnetic laminar mixed convection flow in a vertical channel with symmetric and asymmetric wall heating conditions considering heat generation or absorption. Umavathi and Pratap Kumar (2011) have presented the mixed convection flow of micropolar fluid in a vertical channel with symmetric and asymmetric wall heating conditions. Later Prasad et al. (2017) have investigated mixed convection fully developed flow in a vertical channel in the presence of thermal radiation and viscous dissipation using the Differential Transform Method (DTM) and regular perturbation method.

Studies associated with the magnetohydrodynamic (MHD) flow and heat transfer have received considerable attention because of its immense applications in various branches of industry, science, and technology such as astrophysics, magnetohydrodynamic pumps, magnetohydrodynamic generators, magnetohydrodynamic flow meters, Fusion reactors, etc. A magnetic field applied in the transverse direction of the flow act promptly on the velocity of the fluid particles. The behavior of flow firmly relies upon the orientation and strength of the magnetic field. Hartmann (1937) experimentally and theoretically investigated MHD channel flow with the transverse magnetic field. Poot (1961) and Sparrow et at. (1961) have studied the effect of a magnetic field on free convection heat transfer. Umavathi and Malashetty (2005) have been analyzed the MHD mixed convection flow in a vertical channel

taking into account the effect of viscous and ohmic dissipations. Barletta et al. (2008) explored the effect of Joule heating and viscous dissipation on mixed convection flow in a vertical channel. Ghosh et al. (2010) have been investigated hydromagnetic natural convection boundary layer flow in the presence of an induced magnetic field on an infinite vertical plate and obtained an exact solution. In another related work, Singh et al. (2010) have been numerically studied free convection flow in a vertical channel under the influence of an applied magnetic field, including the effect of magnetic induction. Sivaraj and Kumar (2012) have been investigated MHD Mixed Convective Flow of Viscoelastic and Viscous Fluids in a Vertical Porous Channel. Mixed convection MHD flow in a vertical channel filled with nanofluids had been discussed by Das et al. (2015). Numerically, Chen et al. (2015) have investigated heat transfer performance and entropy generation characteristics of mixed convection magnetohydrodynamic (MHD) flow of Al_2O_3–water nanofluid in a vertical asymmetrically heated parallel plate channel. MHD convection fluid flow and heat transfer in an inclined microchannel with heat generation have been analyzed by Zaidi and Ahmad (2017). Recently Jha and Aina (2017, 2018) analyzed MHD natural convection and mixed convection flow in a vertical microporous channel in the presence of an induced magnetic field.

In this paper, the effect of the induced magnetic field on mixed convection flow in a vertical channel with symmetric and asymmetric wall heating conditions is analyzed taking heat generation into account. The governing equations corresponding to the velocity field, induced magnetic field, temperature field are solved analytically for three types of left-right walls thermal conditions. These conditions are isothermal-isothermal, isoflux-isothermal, and isothermal – isoflux thermal wall conditions. The effect of various parameters on the velocity field, induced magnetic field, induced current density profile and Nusselt number is presented and discussed with the aid of graphs.

2. Governing Equations

Consider the fully developed mixed convection flow of a viscous, incompressible, and electrically conducting fluid in a vertical channel in the presence of an induced magnetic field with heat generation. The distance between the vertical plates is L and plates are maintained at either constant temperature or constant heat flux. Where x'-axis is taken vertically upward and y'- axis is normal to the channel with the origin at the center of the channel (Figure 1).

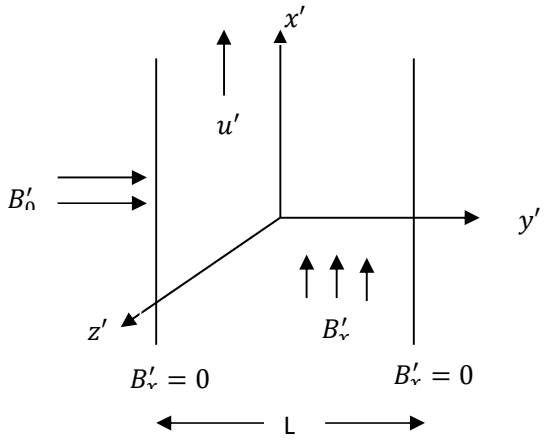

Figure 1. Flow description and coordinate system

A uniform magnetic field of strength $B_0^{'}$ imposed in the direction normal to the flow direction. For a fluid with significant electrical conductivity σ, this in turns induces a magnetic field $B_x^{'}$ along the $x^{'}$-axis. Let $u^{'}$ be the velocity of the fluid along $x^{'}$-axis, then the velocity $\left(u^{'}(\mathrm{y}),0,0\right)$ has only a vertical component and is a function of $y^{'}$ only whereas the magnetic field $\left(B_x^{'},B_0^{'},0\right)$ has component in $x^{'}$ and $y^{'}$ direction respectively. The following assumptions are adopted to facilitate the solution of the governing equations.

1. The flow is steady and laminar.
2. The fluid physical properties are constant, except the density in terms of body force in the momentum equation for which the Boussinesq approximation is invoked.

Under these assumptions the governing equations of the system are

$$-\frac{dP}{dx'}+\nu\frac{d^2u'}{dy'^2}+(\frac{\mu_e B_0'}{\rho})\frac{dB_x'}{dy'}+g\beta(\mathrm{T}-\mathrm{T}_0)=0, \tag{1}$$

$$\left(\frac{1}{\sigma\mu_e}\right)\frac{d^2B_x'}{dy'^2}+B_0'\frac{du'}{dy'}=0, \tag{2}$$

$$\left(\frac{\kappa}{\rho c_p}\right)\frac{d^2T}{dy'^2}+\frac{Q_0}{\rho c_P}\left(T-T_0\right)=0, \tag{3}$$

where u' and T are the fluid velocity and temperature respectively, $P=p+\rho gx$ is the difference between the pressure and hydrostatic pressure. Q_0 is the rate of heat generation. Also for three different wall heating conditions of isothermal-isothermal, isoflux-isothermal, and, isothermal-isoflux a constant pressure gradient $\left(\frac{dP}{dx}=A\right)$ is required for the compatibility of equation (1).

Case I: Isothermal - isothermal walls $\left(T_1-T_2\right)$

Consider that the walls of the channel are isothermal that is the temperature of the boundary at $y'=-\frac{L}{2}$ is T_1, while the temperature at $y'=\frac{L}{2}$ is T_2 $\left(T_1<T_2\right)$. Therefore, the boundary condition for isothermal-isothermal walls can be written as

$$u'(\pm\frac{L}{2})=B_x'(\pm\frac{L}{2})=0,\quad T\left(-\frac{L}{2}\right)=T_1,\quad T\left(\frac{L}{2}\right)=T_2. \tag{4}$$

Introducing the dimensionless variables

$$u=\frac{u'}{u_0},y=\frac{y'}{D},\theta=\frac{T-T_0}{\Delta T},Gr=\frac{g\beta\Delta TD^3}{v^2},\mathrm{Re}=\frac{u_0D}{v},M=\frac{B_0'D}{v}\sqrt{\frac{\mu_e}{\rho}},\phi=\frac{Q_0D^2}{k},$$

$$B = \frac{B_x'}{u_0}\sqrt{\frac{\mu_e}{\rho}},\ \eta = \frac{Gr}{\mathrm{Re}},\ Rt = \frac{T_2 - T_1}{\Delta T},\ Pm = \nu\sigma\mu_e, \tag{5}$$

where $D = 2L$ is the hydraulic diameter, $u_0\left(= -\frac{AD^2}{48\mu}\right)$ is reference velocity and $\Delta T = T_2 - T_1$ is the reference temperature difference, which is different for different wall thermal boundary conditions. For the case of isothermal walls $T_0 = \frac{T_1 + T_2}{2}$. The dimensionless parameter Rt is zero for symmetric wall heating $(T_1 = T_2)$ and Rt is one for asymmetric wall heating $(T_1 < T_2)$ By using the dimensionless variables as defined in Equation. (5), Equations. (1)- (4) can be written as

$$\frac{d^2u}{dy^2} + M\frac{dB}{dy} + \eta\theta + 48 = 0. \tag{6}$$

$$\frac{d^2B}{dy^2} + MPm\frac{du}{dy} = 0. \tag{7}$$

$$\frac{d^2\theta}{dy^2} + \phi.\theta = 0. \tag{8}$$

$$u(\pm\frac{1}{4}) = \mathrm{B}\left(\pm\frac{1}{4}\right) = 0, \quad \theta\left(\pm\frac{1}{4}\right) = \frac{Rt}{2}. \tag{9}$$

Case 2: Isoflux -isothermal walls $(q_1 - T_2)$

For this case, the thermal boundary conditions for the channel walls in the dimensional form can be written as

$$q_1 = -k\left(\frac{dT}{dy'}\right)_{y'=-\frac{L}{2}}, \qquad T\left(\frac{L}{2}\right) = T_2. \tag{10}$$

The dimensionless form of Equation (10) by using Equation (5) with $\Delta T = \frac{q_1 D}{k}$ is given as

$$\left(\frac{d\theta}{dy}\right)_{y=-\frac{1}{4}} = -1, \qquad \theta\left(\frac{1}{4}\right) = R_{qt}, \tag{11}$$

where $R_{qt} = \left(T_2 - T_0\right)/\Delta\mathrm{T}$ is the thermal ratio parameter.

Case 3: Isothermal - isoflux walls $\left(T_1 - q_2\right)$

For this situation, the thermal boundary conditions for the channel walls are

$$T\left(-\frac{L}{2}\right) = T_1 \ , \quad q_2 = -k\left(\frac{dT}{dy'}\right)_{y'=\frac{L}{2}}. \tag{12}$$

The dimensionless form of Equation (12) by using Equation (5) with $\Delta T = \frac{q_2 D}{k}$ is given as

$$\theta\left(-\frac{1}{4}\right) = R_{tq} \ , \qquad \left(\frac{d\theta}{dy}\right)_{y=\frac{1}{4}} = -1, \tag{13}$$

where $R_{tq} = \left(T_1 - T_0\right)/\Delta T$ is the thermal ratio parameter.

3. Analytical Solutions

Case 1: Isothermal-isothermal walls

The solutions of Equations (6)-(8) with boundary conditions (9) are

$$\theta = \frac{Rt}{2}\frac{\sin\sqrt{\phi}y}{\sin\sqrt{\phi}/4}. \tag{14}$$

$$u = a_1 + a_2\cosh\left(M\sqrt{Pm}y\right) + a_3\sinh\left(M\sqrt{Pm}y\right) + \frac{\eta Rt}{2\left(\phi + M^2 Pm\right)}.\frac{\sin\left(\sqrt{\phi}y\right)}{\sin(\sqrt{\phi}/4)}. \tag{15}$$

$$\begin{aligned} B = &\left[\frac{\eta M\ Pm\, Rt}{2\sqrt{\phi}\left(\phi + \mathrm{M}^2\ \mathrm{Pm}\right)}\right].\frac{\cos\left(\sqrt{\phi}y\right)}{\sin\left(\sqrt{\phi}/4\right)} - a_2\sqrt{Pm}\sinh\left(M\sqrt{Pm}y\right) \\ &- \frac{\eta M\ Pm\, Rt}{2\sqrt{\phi}\left(\phi + M^2 Pm\right)}\cos\left(\sqrt{\phi}/4\right) - a_3\sqrt{Pm}\cosh\left(M\sqrt{Pm}\ y\right) \\ &+ a_3\sqrt{Pm}\ \cosh\left(M\sqrt{Pm}/4\right) - \frac{48}{M}y. \end{aligned} \tag{16}$$

The induced current density is given by

$$J = -\left(\frac{dB}{dy}\right).$$

$$= M\sqrt{Pm\,\phi}\left\{a_2\cosh\left(M\sqrt{\phi}y\right)+a_3\sinh\left(M\sqrt{\phi}y\right)\right\}+\left\{\frac{\eta\,M\,Pm\,Rt}{2\left(\phi+M^2\,Pm\right)}\right\} \times\frac{\sin\left(\sqrt{\phi}y\right)}{\sin\left(\sqrt{\phi}/4\right)}+\frac{48}{M}. \tag{17}$$

Case 2: Isoflux-isothermal walls

The solutions of Equations (6) - (8) by using the boundary conditions (11) are given as

$$\theta = b_1\sin\left(\sqrt{\phi}y\right)+b_2\cos(\sqrt{\phi}\,\mathrm{y}). \tag{18}$$

$$u = b_5\sinh\left(M\sqrt{Pm}y\right)+\left(\frac{\eta}{\phi+M^2Pm}\right)\left\{b_1\sin\left(\sqrt{\phi}y\right)+b_2\cos\left(\sqrt{\phi}y\right)\right\} +b_3+b_4\cosh\left(M\sqrt{Pm}y\right). \tag{19}$$

$$B = -\sqrt{Pm}\left\{b_4\sinh\left(M\sqrt{Pm}y\right)+b_5\cosh\left(M\sqrt{Pm}y\right)\right\}+\sqrt{Pm}\,b_5\cosh\left(M\sqrt{Pm}/4\right) +\left(\frac{M\,Pm}{\sqrt{\phi}}\right)\left(\frac{\eta}{\phi+M^2Pm}\right)\left\{b_1\cos\left(\sqrt{\phi}y\right)-b_2\sin\left(\sqrt{\phi}y\right)\right\} -\left\{\frac{\eta M\,Pm\,b_1}{\sqrt{\phi}\left(\phi+M^2Pm\right)}\right\}\cos\left(\sqrt{\phi}/4\right)-\frac{48}{M}y. \tag{20}$$

The induced current density is given by

$$J = -\frac{dB}{dy}. = M\,Pm\left\{b_4\cosh\left(M\sqrt{Pm}y\right)+b_5\sinh\left(M\sqrt{Pm}y\right)\right\}+\frac{48}{M} +\left(\frac{M\,Pm\,\eta}{\phi+M^2Pm}\right)\left\{b_1\sin\left(\sqrt{\phi}y\right)-b_2\cos\left(\sqrt{\phi}y\right)\right\}. \tag{21}$$

Case 3: Isothermal -isoflux-walls

The solutions for Equations. (6) - (8) with the boundary conditions (13) are

$$\theta = c_1\sin\left(\sqrt{\phi}y\right)+c_2\cos(\sqrt{\phi}\,\mathrm{y}). \tag{22}$$

$$u = c_5 \sinh\left(M\sqrt{Pm}\,y\right) + \left(\frac{\eta}{\phi + M^2 Pm}\right)\left\{c_1 \sin\left(\sqrt{\phi}\,y\right) + c_2 \cos\left(\sqrt{\phi}\,y\right)\right\} + c_4 \cosh\left(M\sqrt{Pm}\,y\right) + c_3 \ . \tag{23}$$

$$B = -\sqrt{Pm}\left\{c_4 \sinh\left(M\sqrt{Pm}\,y\right) + c_5 \cosh\left(M\sqrt{Pm}\,y\right)\right\} + \sqrt{Pm}\,c_5 \cosh\left(M\sqrt{Pm}/4\right) + \left(\frac{M\,Pm}{\sqrt{\phi}}\right)\left(\frac{\eta}{\phi + M^2 Pm}\right)\left\{c_1 \cos\left(\sqrt{\phi}\,y\right) - c_2 \sin\left(\sqrt{\phi}\,y\right)\right\} - \left\{\frac{\eta M\,Pm\,c_1}{\sqrt{\phi}\left(\phi + M^2 Pm\right)}\right\}\cos\left(\sqrt{\phi}/4\right) - \frac{48}{M}y. \tag{24}$$

The induced current density is given by

$$J = -\left(\frac{dB}{dy}\right). = M\,Pm\left\{c_4 \cosh\left(M\sqrt{Pm}\,y\right) + c_5 \sinh\left(M\sqrt{Pm}\,y\right)\right\} + \left(\frac{M\,Pm\,\eta}{\phi + M^2 Pm}\right)\left\{c_1 \sin\left(\sqrt{\phi}\,y\right) + c_2 \cos\left(\sqrt{\phi}\,y\right)\right\} + \frac{48}{M}. \tag{25}$$

4. Rate of Heat Transfer

It is of practical interest and significant to enumerate the Nusselt number between the fluid and plates. The Nusselt number at each channel wall for three different thermal boundary conditions is defined as

Isothermal -isothermal walls $\left(T_1 - T_2\right)$

$$N_1 = \frac{h_1 D}{k} = \frac{D}{\Delta T}\left(\frac{dT}{dy}\right)_{-L/2} = \left.\frac{d\theta}{dy}\right|_{y=-1/4}, \tag{26}$$

$$N_2 = \frac{h_2 D}{k} = \frac{D}{\Delta T}\left(\frac{dT}{dy}\right)_{L/2} = \left.\frac{d\theta}{dy}\right|_{y=1/4}, \tag{27}$$

where N_1 and N_2 are the Nusselt numbers at the left and right walls respectively. For this case, the Nusselt numbers are given as

$$N_1 = N_2 = \frac{Rt\sqrt{\phi}\cos\left(\sqrt{\phi}/4\right)}{\sin\left(\sqrt{\phi}/4\right)}. \tag{28}$$

Isoflux -isothermal walls $(q_1 - T_2)$

$$N_1 = \frac{h_1 D}{k} = \frac{Dq_1}{k(T_1 - T_0)} = \frac{1}{\theta_1}, \tag{29}$$

$$N_2 = \frac{h_2 D}{k} = \frac{D}{\Delta T}\left(\frac{dT}{dy}\right)_{L/2} = \theta_2', \tag{30}$$

where the subscripts 1 and 2 denote the Nusselt numbers at the left and right walls respectively and given by the Equations (29) and (30) as

$$N_1 = -\frac{1}{b_1 \sin\left(\sqrt{\phi}/4\right) - b_2 \cos\left(\sqrt{\phi}/4\right)}. \tag{31}$$

$$N_2 = \sqrt{\phi}\left\{b_1 \cos\left(\sqrt{\phi}/4\right) - b_2 \sin\left(\sqrt{\phi}/4\right)\right\}. \tag{32}$$

Isothermal - isoflux walls $(T_1 - q_2)$

$$N_1 = \frac{h_1 D}{k} = \frac{D}{\Delta T}\left(\frac{dT}{dy}\right)_{-L/2} = \theta_1'. \tag{33}$$

$$N_2 = \frac{h_2 D}{k} = \frac{Dq_2}{k(T_2 - T_0)} = \frac{1}{\theta_2}. \tag{34}$$

In this case, Equations (33) and (34) provides the following Nusselt numbers

$$N_1 = \sqrt{\phi}\left\{c_1 \cos\left(\sqrt{\phi}/4\right) + c_2 \sin\left(\sqrt{\phi}/4\right)\right\}. \tag{35}$$

$$N_2 = \frac{1}{c_1 \sin\left(\sqrt{\phi}/4\right) + c_2 \cos\left(\sqrt{\phi}/4\right)}. \tag{36}$$

5. Results and Discussion

In this paper, the effect of the induced magnetic field on mixed convection flow in a vertical channel with symmetric and asymmetric wall heating conditions is analyzed taking heat generation into account. The following conclusions based on graphs are drawn.

Figure 2 depicts the velocity distribution in a vertical channel with asymmetric isothermal – isothermal wall heating conditions for various values of Hartmann number M and two chosen values of the mixed convection parameter $\eta = \pm 200$. It is clear from the graph that for the buoyancy opposing flow $(\eta = -200)$ and buoyancy assisting flow $(\eta = 200)$ a flow reversal condition takes place near to the left and right wall of the channel, respectively. It seems that

the magnitude of the velocity of fluid particles decreases with the increase of Hartmann number M. Physically, the presence of a transverse magnetic field in an electrically conducting fluid gives rise to the magnetic Lorentz force, which is a retarding force on the velocity field. The effect of heat generation coefficient ϕ and magnetic Prandtl number Pm on the velocity profile for isothermal-isothermal wall heating conditions is evident in Figure 3. As the heat generation coefficient ϕ increases, the velocity of fluid particles decreases and reversed flow occurs close to the isothermal walls for $\eta = \pm 200$. It is also shown in the graph that as the value of Pm increases the velocity of fluid particles decreases. Figure 4 illustrates the variation of the induced magnetic field with the heat generation coefficient ϕ and the magnetic Prandtl number Pm. It is observed that the induced magnetic field increases with the increasing magnetic Prandtl number Pm. The induced magnetic field also increases as the heat generation coefficient ϕ decreases for $\eta = \pm 200$. Figure 5 shows that as the value of Hartmann number M increases the induced magnetic field increases for both the buoyancy aiding flow ($\eta = 200$) and buoyancy opposing flow ($\eta = -200$).

Figures 6 and 7 display the variation of a velocity profile for the values of Hartmann number M, heat generation coefficient ϕ and magnetic Prandtl number Pm for isoflux-isothermal wall heating conditions. As the value of Hartmann number M increases the velocity of fluid particles decreases and the direction of flow is upward for buoyancy adding flow ($\eta = 200$) and downward for buoyancy opposing flow ($\eta = -200$). The effect of the heat generation coefficient ϕ and magnetic Prandtl number Pm shown in Figure 7. It is clear from Figure 7 that the velocity of fluid particles increases with the increase of heat generation coefficient ϕ and decrease of magnetic Prandtl number Pm for $\eta = \pm 200$.

The effect of the heat generation coefficient ϕ and induced magnetic field parameter Pm is shown in Figure 8. As the value of ϕ increases, the induced magnetic field increases for $\eta = 200$ (upward flow) from $y = -0.25$ to $y = -0.05$ and reverses its direction from $y = -0.05$ to $y = 0.25$ while for $\eta = -200$ downward flow occurs. The magnitude of the induced magnetic field is large for the value of $Pm = 0.5$. Figure 9 shows the effect of Hartmann number M on the induced magnetic field. The value of the induced magnetic field increases with the increase in the value of M.

Figures 10 and 11 depict the variation of a velocity profile for the various values of Magnetic Prandtl number Pm, heat generation coefficient ϕ, and Hartmann number M in the isothermal-isoflux wall heating conditions. The velocity of fluid particles increases as ϕ increases in the downward direction for $\eta = -200$ and upward for $\eta = 200$. Also, the velocity of fluid particles decreases with the increase of Hartmann number M for $\eta = \pm 200$. The magnetic field profile for the values of the magnetic Prandtl number Pm, heat generation coefficient ϕ and Hartmann Number M observed in Figures 12 and 13.

Figures 14 and 15 illustrate the effect of magnetic Prandtl number Pm and Hartmann number M on induced current density for the isothermal-isothermal wall heating condition respectively. It is evident from the graphs that the induced current density increases on the increase of magnetic Prandtl number Pm and Hartmann number M and reversed flow occurs at the isothermal walls for $\eta = \pm 200$.

The effect of Pm and M on the induced current density is illustrated in Figures 16 and 17, respectively. As the value of Pm and M increases the induced current density increases and its direction is upward for $\eta = 200$ and downward for $\eta = -200$. In Figures 18 and 19, the profile of induced current density shows a similar behavior as shown in the heat flux-isothermal case. It is also clear from Figures 14-19 that there exist points of intersection inside the vertical channel where the induced current density is independent of Hartmann number and magnetic Prandtl number.

Figures 20, 21, 22 depicts the variation of rate of heat transfer with the heat generation coefficient and thermal ratio parameter (Rt, Rqt and Rtq) for isothermal-isothermal, isoflux –isothermal, and isothermal-isoflux cases. It is clear from Figure 20 that in case of isothermal-isothermal wall heating conditions Nusselt number at the cold wall (or hot wall) increases with the increase in the value of the thermal ratio parameter Rt and decreases as the value of ϕ increases. It is also observed that the magnitude of the rate of heat transfer on the isoflux channel wall decreases with the increase of heat generation coefficient ϕ and thermal ratio parameter Rqt whereas, an increase in the value of ϕ and Rqt increases the rate of heat transfer on the isothermal channel wall (See Figure 21). The reverse is the case for the isothermal-isoflux, wall heating conditions (See Figure 22). However, for the isoflux-isothermal and isothermal-isoflux case, the Nusselt number is constant at $\phi = 0$ for all values of Rqt and Rtq.

6. Conclusion

The present study leads to the following conclusions:

1. The velocity of fluid particles decreases with the increase of heat generation coefficient in case of isothermal - isothermal wall heating conditions while it is increased with the increase of heat generation coefficient in case of isoflux- isothermal and isothermal-isoflux wall heating conditions. It is also found that the velocity of fluid particles decreases with the increasing of Hartmann number and magnetic Prandtl number.
2. Increasing the value of magnetic Prandtl number and Hartmann number causes an enhancement in the induced magnetic field.
3. It is also observed that induced current density increases on increasing magnetic Prandtl number and Hartmann number.
4. The magnitude of the rate of heat transfer on the isoflux channel wall decreases with the increase of heat generation coefficient ϕ and thermal ratio parameter Rqt whereas, an increase in the value of ϕ and Rqt increases the rate of heat transfer on the isothermal channel wall.

REFERENCES

Aung, W. and Worku, G. (1986). Theory of fully developed combined convection including flow reversal, ASME j. Heat Transfer, Vol. 108, pp. 458-488.

Aung, W. and Worku, G. (1986). Developing flow and flow reversal in a vertical channel with asymmetric wall temperatures, ASME j. Heat Transfer, Vol. 108, pp. 229-304.

Aung, W. and Worku, G. (1987). Mixed convection in ducts with asymmetric wall temperatures, ASME j. Heat Transfer, Vol. 109, pp. 947-951.

Barletta, A. and Celli, M. (2008). Mixed convection MHD flow in a vertical channel: effect of Joule heating and viscous dissipation, Int. J. Of heat and mass transfer, Vol. 51(25-26) pp. 6110-6117.

Chamkha, A. J. (2002). On laminar hydromagnetic convection flow in a vertical channel with symmetric and asymmetric wall heating conditions, Int. J. Heat and Mass Transfer, Vol. 45, pp. 2509-2525.

Cheng, C.H., Kou, H.S. and Huang, W.H. (1990). Flow reversal and heat transfer of fully developed mixed convection in a vertical channel, J. of Thermophysics and heat transfer, Vol. 4(3), pp. 375-383.

Chen, C.K., Chen, B.S. and Liu, C.C. (2015). Entropy generation in mixed convection magnetohydrodynamic nanofluid flow in vertical channel, International Journal of Heat and Mass Transfer, Vol. 91, pp. 1026-1033.

Das, S., Jana, R. N. and Makinde, O.D. (2015). Mixed convection Magnetohydrodynamic flow in a vertical channel filled with nanofluids, Engg. Science and technology, an Int. Journal, Vol. 18(2), pp. 244-255.

Ghosh, S.K., Beg, O.A. and Zueco, J. (2010). Hydromagnetic free convection flow with induced magnetic field effect, Meccanica, Vol.14, pp. 175-185.

Hartmann, J. (1937). Hg-dynamics I theory of the laminar flow of an electrically conductive liquid in a homogenous magnetic field, Det Kal. Danske Videnskabernesselskab, Mathematisk-fysiske Meddeleser. XV:1-27

Jha, B.K. and Aina, B. (2017). Effect of Induced Magnetic Field on MHD Mixed Convection Flow in Vertical Microchannel. International Journal of Applied Mechanics and Engineering 22(3) pp. 567-582.

Jha, B.K. and Aina, B. (2018). Magnetohydrodynamic natural convection flow in a Vertical micro-porous-channel in the presence of induced magnetic field, Commun. Nonlinear Sci Numer Simulat, Vol. 64, pp. 14-34.

Ostrach, S. (1954). Combined Natural and Forced Convection Laminar Flow and Heat Transfer of Fluids With and Without Heat Sources in Channels with Linearly Varying Wall Temperature, NACA Technical Note No. 3141.

Poots, G (1961). Laminar natural convection flow in magneto-hydrodynamics, Int. J. Heat and mass transfer, Vol. 3(1), pp. 1-25

Parsad, K. V., Mallikarjun, P. and Vaidya, H. (2017). Mixed Convection fully developed flow in a vertical channel in the presence of thermal radiation and viscous dissipation, Int. J. of Applied Mechanics and Engineering, Vol.22(1), pp.123-144

Sparrow, E.M. and Cess, R. D. (1961). The effect of a magnetic field on free convection heat transfer, Int. J of Heat and Mass Transfer, Vol.3(4), pp. 267-274.

Singh, R.K., Singh, A.K., Sachati, N.C. and Chandran, P. (2010). On Hydromagnetic free convection in the presence of induced Magnetic field, Heat and Mass Transfer, Vol. 46, pp. 523-529.

Sivaraj, R. and Kumar, B. R. (2012). MHD Mixed Convective Flow of Viscoelastic and Viscous Fluids in a Vertical Porous Channel, Applications and Applied Mathematics, Vol. 7(1), pp. 99-116.

Umavathi, J.C. and Malashetty, M. S. (2005). Magnetohydrodynamic mixed convection in a vertical channel, Int. J. of non-linear mechanics, Vol. 40(1), pp. 91-101.

Umavathi, J.C. and Kumar, J.P. (2011). Mixed convection flow of Micropolar fluid in a vertical channel with symmetric and asymmetric wall heating conditions, Int. J Applied Mechanics and Engineering, Vol. 16(1), pp.141-159.

Zaidi, H. N. and Ahmad, N. (2017). MHD Convection Fluid Flow and Heat Transfer in an Inclined Microchannel with Heat Generation, American Journal of Applied Mathematics,Vol.5(5), pp. 124-131.

APPENDIX

$$a_1 = -a_2 \cosh\left(M\sqrt{Pm}/4\right),\ a_2 = -\frac{12}{M\sqrt{Pm}\sinh\left(M\sqrt{Pm}/4\right)}$$

$$a_3 = -\frac{\eta Rt}{2\left(\phi + M^2 Pm\right)}.\frac{1}{\sinh\left(M\sqrt{Pm}/4\right)},\ b_1 = -\frac{\left\{\cos\left(\sqrt{\phi}/4\right) + 0.5Rt\sqrt{\phi}\sin\left(\sqrt{\phi}/4\right)\right\}}{\sqrt{\phi}\cos\left(\sqrt{\phi}/2\right)}$$

$$b_2 = \frac{\left\{\sin\left(\sqrt{\phi}/4\right) + 0.5Rt\sqrt{\phi}\cos\left(\sqrt{\phi}/4\right)\right\}}{\sqrt{\phi}\cos\left(\sqrt{\phi}/2\right)},\ b_3 = -b_4\cosh\left(M\sqrt{Pm}/4\right) - \frac{\eta b_2}{\phi + M^2 Pm}\cos\left(\sqrt{\phi}/4\right)$$

$$b_4 = -\frac{12}{M\sqrt{Pm}\sinh\left(M\sqrt{Pm}/4\right)} - \frac{1}{\sqrt{\phi}}\left(\frac{\eta M\sqrt{Pm}\, b_2}{\phi + M^2 Pm}\right)\left\{\frac{\sin\left(\sqrt{\phi}/4\right)}{\sinh\left(M\sqrt{Pm}/4\right)}\right\}$$

$$b_5 = -\left(\frac{\eta b_1}{\phi + M^2 Pm}\right)\left\{\frac{\sin\left(\sqrt{\phi}/4\right)}{\sinh\left(M\sqrt{Pm}/4\right)}\right\},\ b_6 = \frac{\left\{0.5Rt\sqrt{\phi}\cosh\left(\sqrt{\phi}/4\right) + \sinh\left(\sqrt{\phi}/4\right)\right\}}{\sqrt{\phi}\cosh\left(\sqrt{\phi}/2\right)}$$

$$b_7 = \frac{\left\{0.5Rt\sqrt{\phi}\sinh\left(\sqrt{\phi}/4\right) - \cosh\left(\sqrt{\phi}/4\right)\right\}}{\sqrt{\phi}\cosh\left(\sqrt{\phi}/2\right)},\ b_8 = \left(\frac{\eta b_6}{\phi - M^2 Pm}\right)\cosh\left(\sqrt{\phi}/4\right) - b_9\cosh\left(M\sqrt{Pm}/4\right)$$

$$b_9 = -\frac{12}{M\sqrt{Pm}\sinh\left(M\sqrt{Pm}/4\right)} + \frac{1}{\sqrt{\phi}}\left(\frac{\eta M\sqrt{Pm}\, b_2}{\phi - M^2 Pm}\right)\left(\frac{\sinh\left(\sqrt{\phi}/4\right)}{\sinh\left(M\sqrt{Pm}/4\right)}\right)$$

$$b_{10} = \left(\frac{\eta b_7}{\phi - M^2 Pm}\right)\left\{\frac{\sin\left(\sqrt{\phi}/4\right)}{\sinh\left(M\sqrt{Pm}/4\right)}\right\}$$

$$c_1 = \frac{\left\{0.5Rt\sqrt{\phi}\sin\left(\sqrt{\phi}/4\right) - \cos\left(\sqrt{\phi}/4\right)\right\}}{\sqrt{\phi}\cos\left(\sqrt{\phi}/2\right)},\ c_2 = \frac{\left\{0.5Rt\sqrt{\phi}\cos\left(\sqrt{\phi}/4\right) - \sin\left(\sqrt{\phi}/4\right)\right\}}{\sqrt{\phi}\cos\left(\sqrt{\phi}/2\right)}$$

$$c_3 = -c_4\cosh\left(M\sqrt{Pm}/4\right) - \frac{\eta c_2}{\phi + M^2 Pm}\cos\left(\sqrt{\phi}/4\right)$$

$$c_4 = -\frac{12}{M\sqrt{Pm}\sinh\left(M\sqrt{Pm}/4\right)} - \frac{1}{\sqrt{\phi}}\left(\frac{\eta M\sqrt{Pm}\, c_2}{\phi + M^2 Pm}\right)\left\{\frac{\sin\left(\sqrt{\phi}/4\right)}{\sinh\left(M\sqrt{Pm}/4\right)}\right\}$$

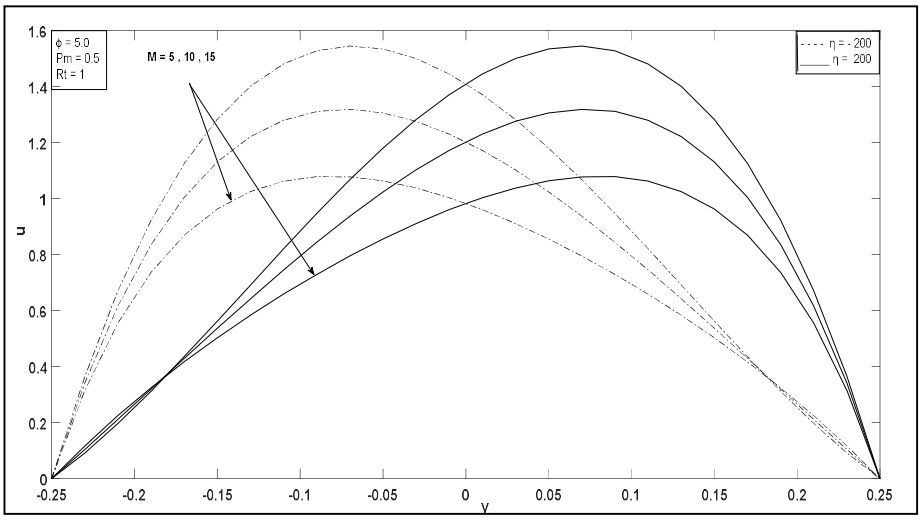

Figure 2. Effect of Hartmann number (M) on velocity profile for $(T_1 - T_2)$ case

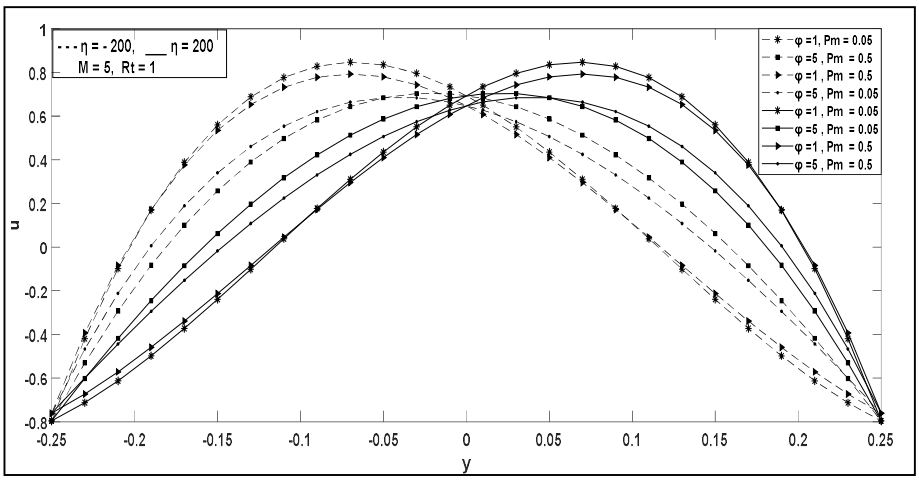

Figure 3. Effect of ϕ and Pm on Velocity profile for $(T_1 - T_2)$ case

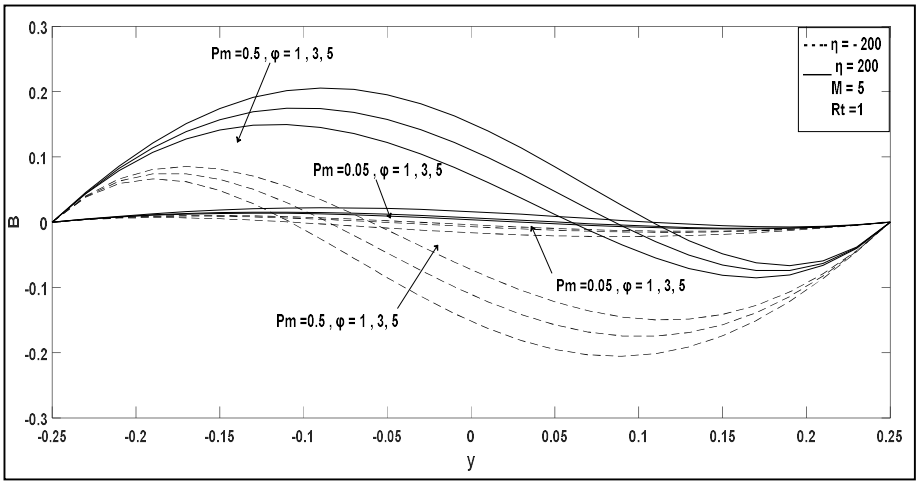

Figure 4. Effect of ϕ and Pm on induced magnetic field for $(T_1 - T_2)$ case

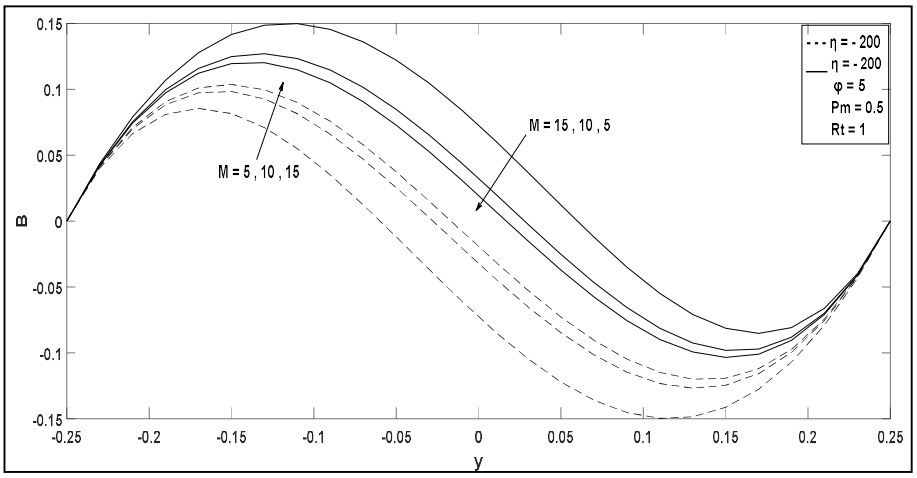

Figure 5. Effect of Hartmann number (M) on induced magnetic field for $(T_1 - T_2)$ case

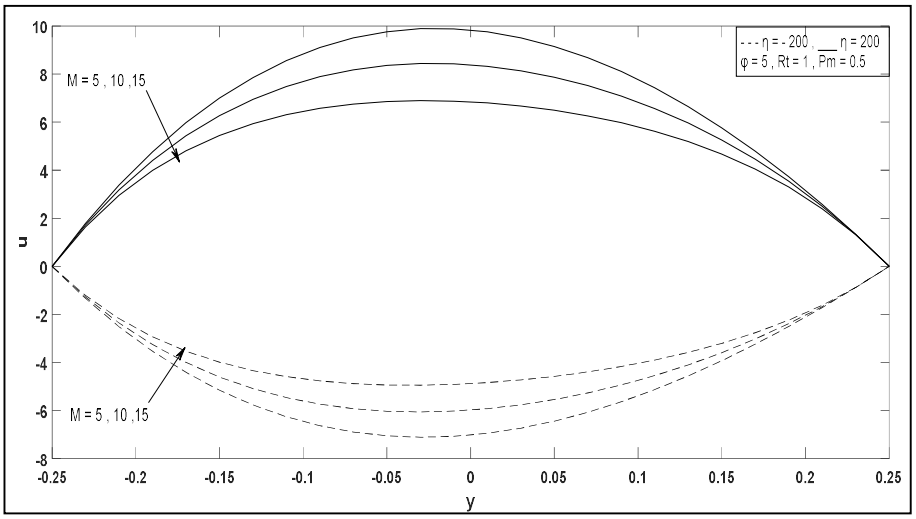

Figure 6. Effect of Hartmann Number M on velocity profile for $(q_1 - T_2)$ case

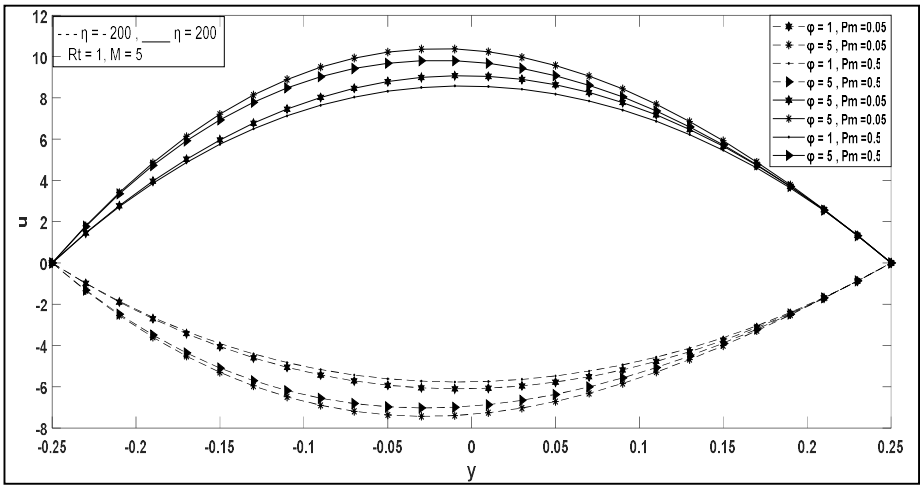

Figure 7. Effect of ϕ and Pm on Velocity profile for $(q_1 - T_2)$ case

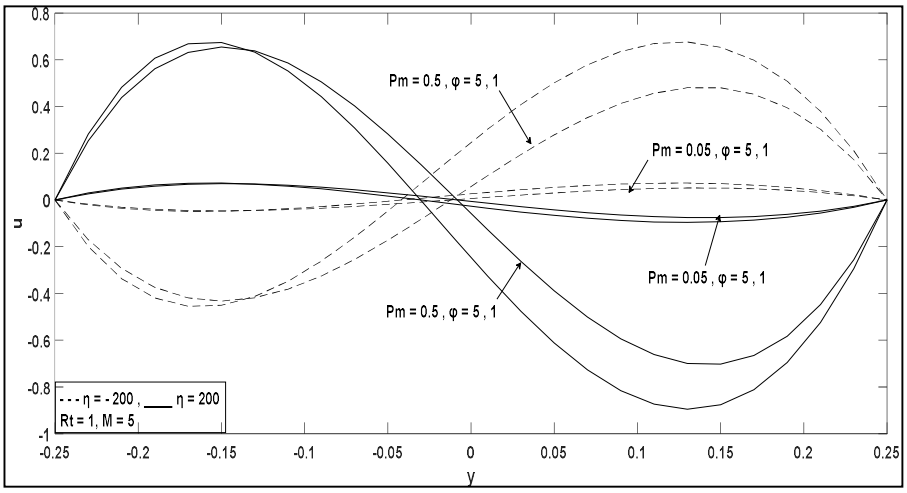

Figure 8. Effect of ϕ and Pm on Magnetic field profile for $(q_1 - T_2)$ case

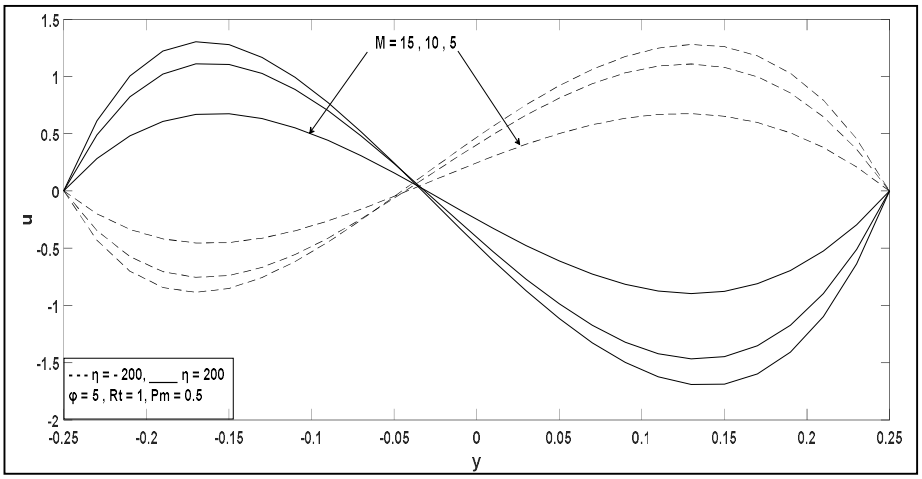

Figure 9. Effect Hartmann Number M on Magnetic field profile for $(q_1 - T_2)$ case

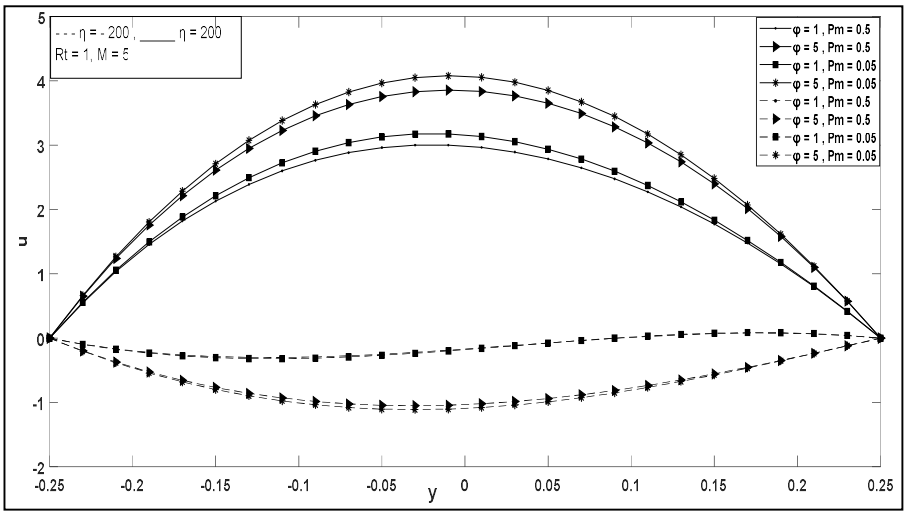

Figure 10. Effect of ϕ and Pm on Velocity profile for $(T_1 - q_2)$ case

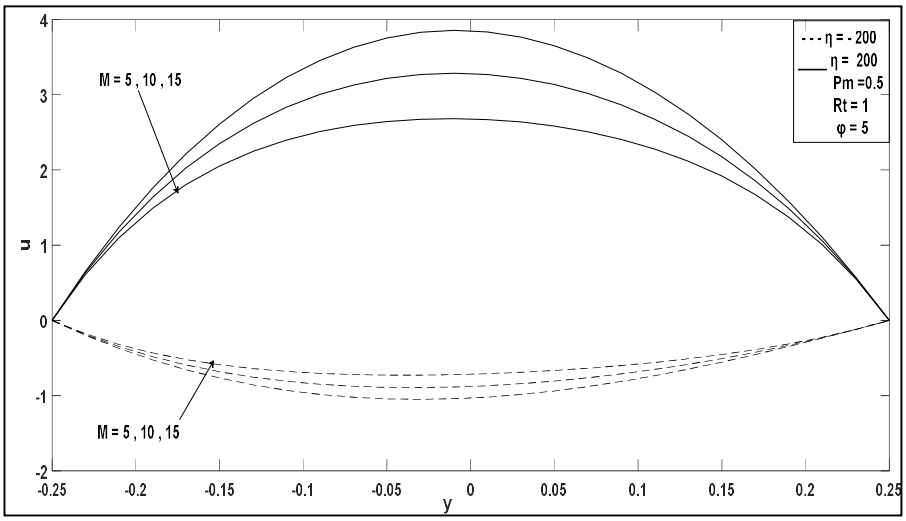

Figure 11. Effect of Hartmann number (M) on velocity profile for $(T_1 - q_2)$ case

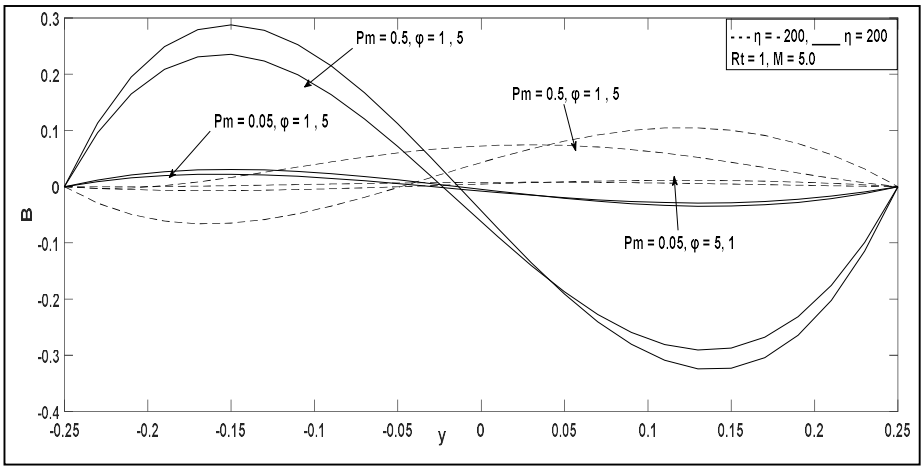

Figure 12. Effect of ϕ and Pm on Magnetic field profile for $(T_1 - q_2)$ case

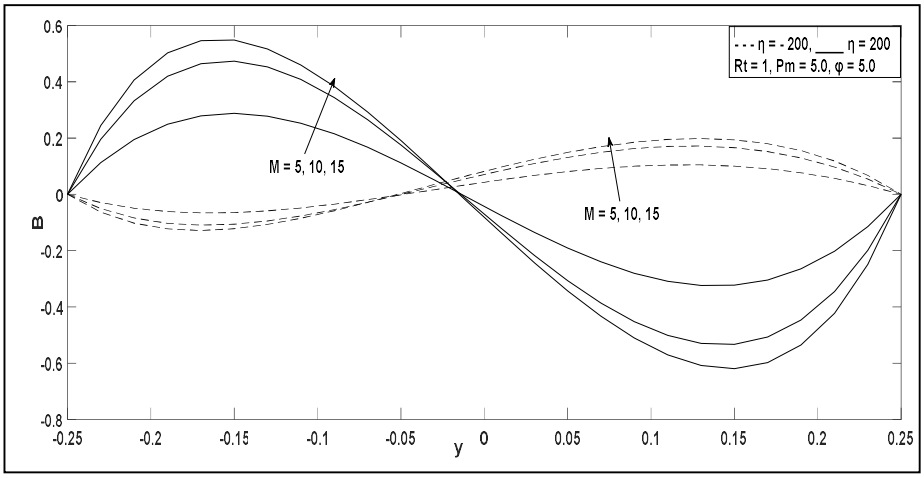

Figure 13. Effect of Hartmann number (M) on Magnetic field profile for $(T_1 - q_2)$ case

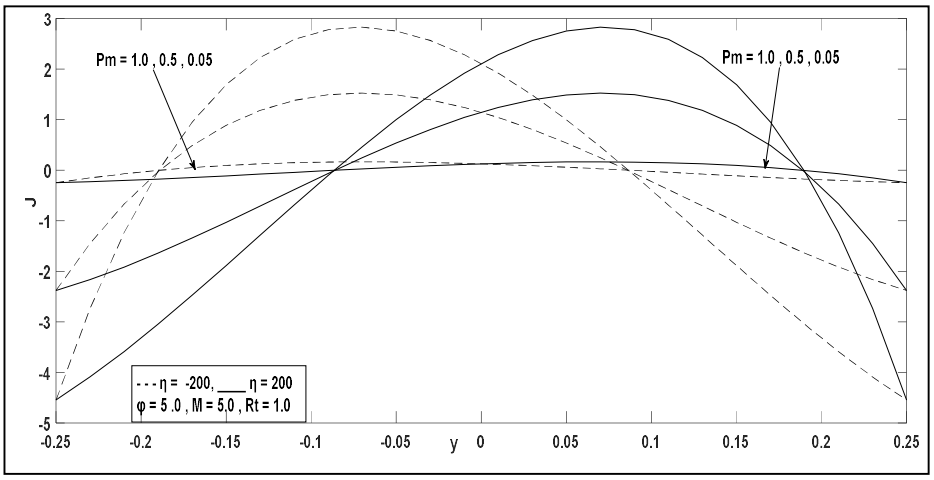

Figure 14. Effect of Pm on induced current density for $(T_1 - T_2)$ case

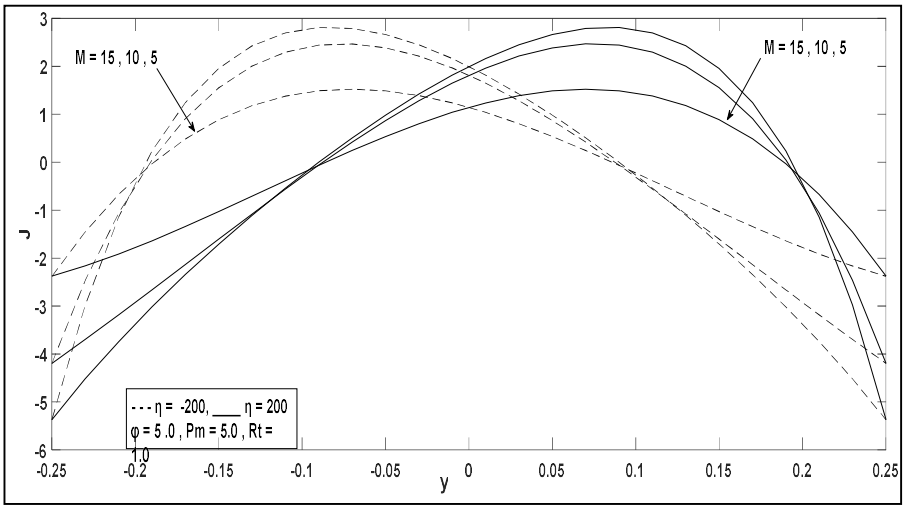

Figure 15. Effect of M on induced current density for $(T_1 - T_2)$ case

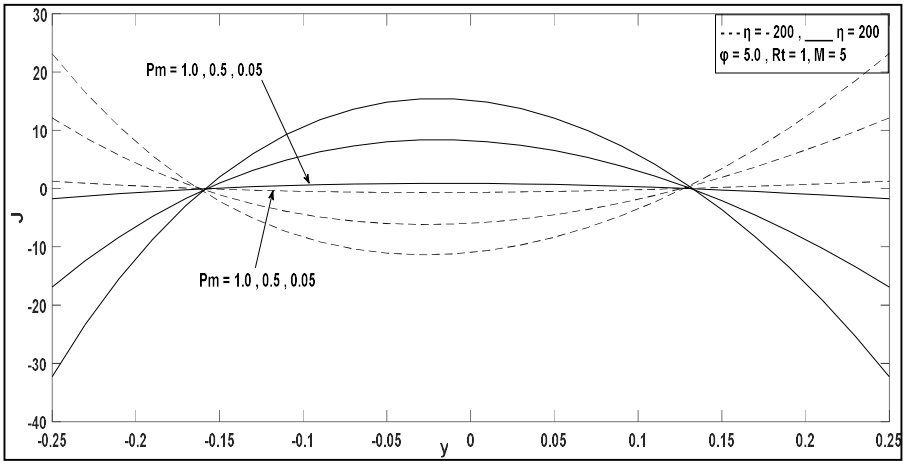

Figure 16. Effect of Pm on induced current density for $(q_1 - T_2)$ case

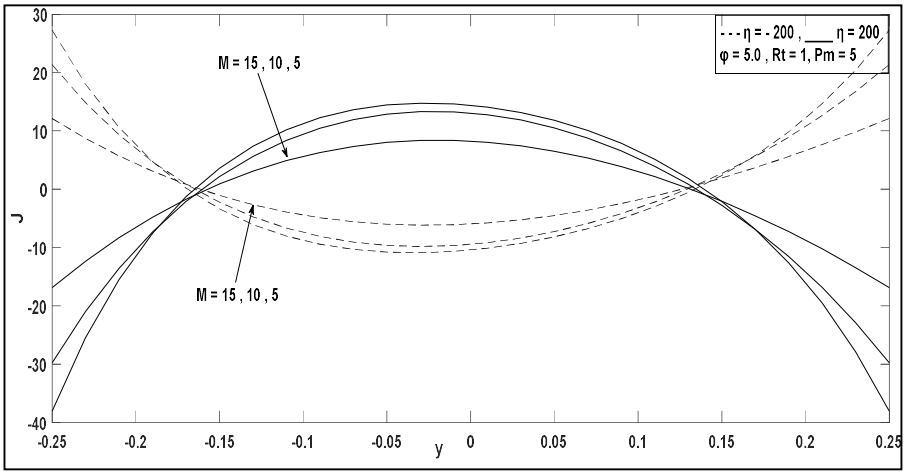

Figure 17. Effect of M on induced current density for $(q_1 - T_2)$ case

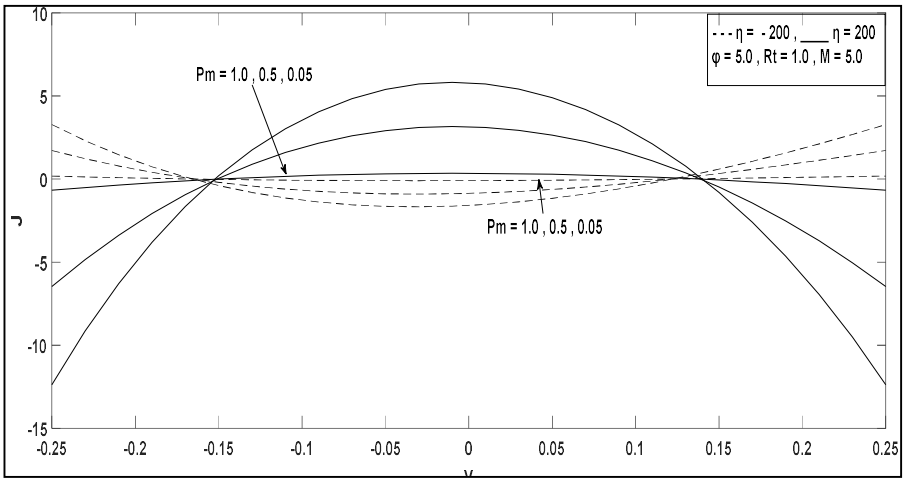

Figure 18. Effect of Pm on induced current density for $(T_1 - q_2)$ case

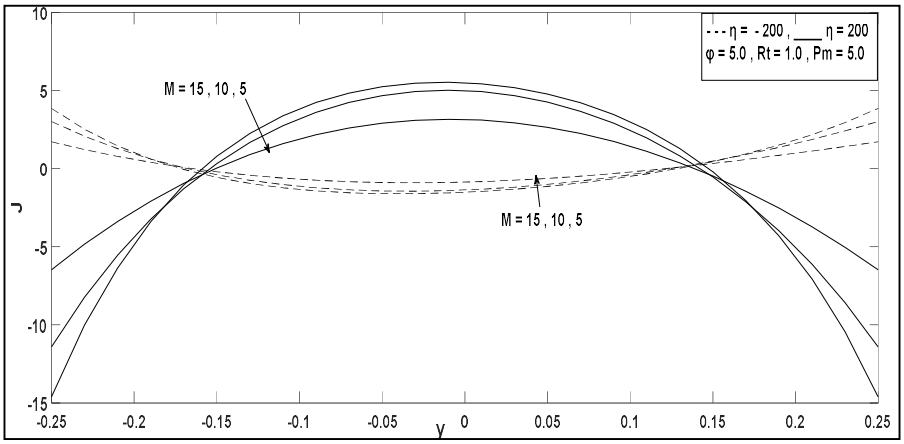

Figure 19. Effect of M on induced current density for $(T_1 - q_2)$ case

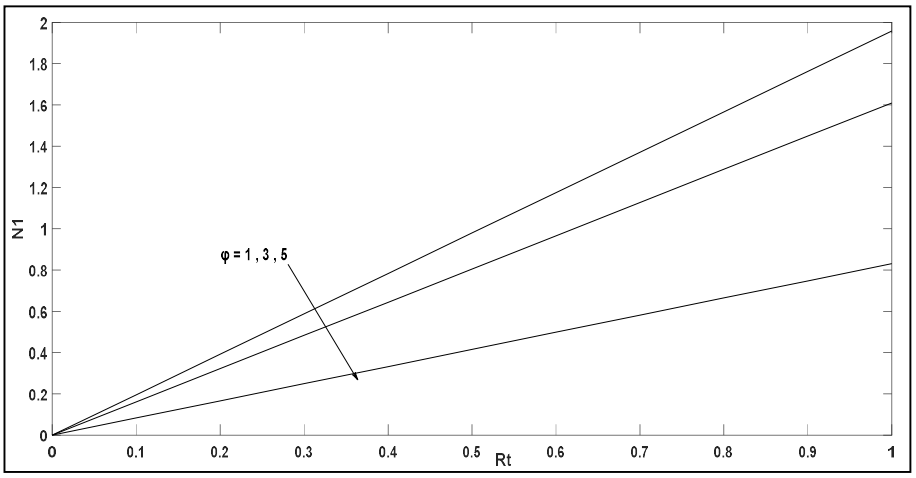

Figure 20. Effect of Rt and ϕ on Nusselt number

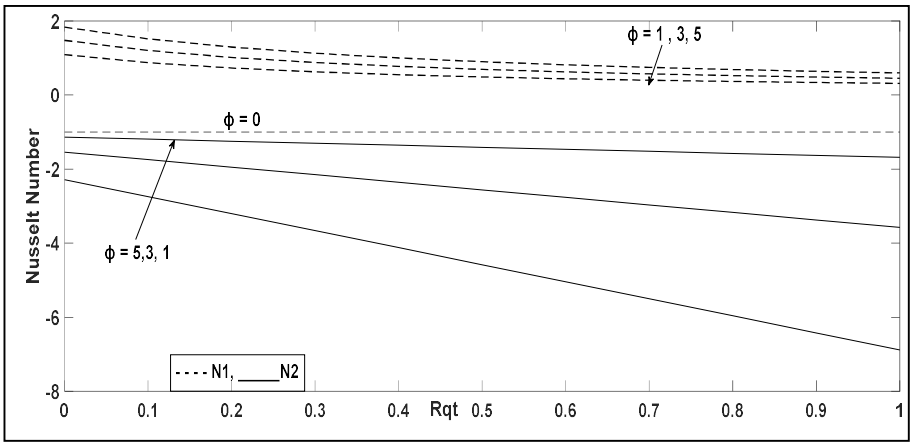

Figure 21. Effect of Rqt and ϕ on Nusselt number

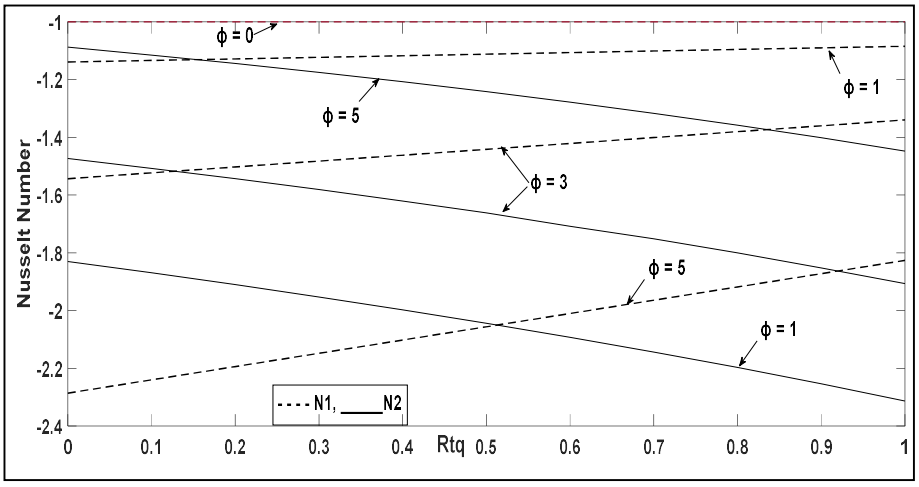

Figure 22. Effect of Rtq and ϕ on Nusselt number

Bibliography:

Hasan Nihal Zaidi got his Ph.D. in Mathematics from Jamia Millia Islamia University, Delhi, India in 2006. He is presently an Assistant professor at the Department of Basic Science at the University of Hail, Saudi Arabia. He had 14 years of teaching experience in graduate and undergraduate students. His research area of interest is Couple stress fluid flows, Heat and, Mass Transfer, MHD fluid flows and Fluid Dynamics.